

Investigation of avalanche photo diodes in NPI Rez in frame of collaboration work with JINR in 2014

V. Kushpil^{1,a}, V. Mikhaylov^{2,a,b}, S. Kushpil^a, O. Svoboda^a, P. Tlustý^a, A. Kugler^a,
V. Ladygin^c

^a*Nuclear Physics Institute, Academy of Sciences of the Czech Republic, Řež, Czech Republic*

^b*Czech Technical University in Prague, Faculty of Nuclear Sciences and Physical Engineering, Prague, Czech Republic*

^c*Joint Institute of Nuclear Research, Laboratory of High Energy Physics, Dubna, Russian Federation*

E-mail: ¹kushpil@ujf.cas.cz; ²mikhaylov@ujf.cas.cz

Modern APD with high gain known as SiPM, MPPC, G-APD are well candidates for hadron and electromagnetic calorimetry for CBM (FAIR) and BM@N (NICA) projects. In collaboration with LHE/JINR group, we started the project with the goals of APD type selection, readout optimization and sophisticated data analysis. One of the main tasks is the APD radiation hardness studies to understanding their behaviour in radiation environment compared to the normal conditions. We present results of investigation of Zekotec, KETEK, Hamamatsu APDs and furthermore results of investigation of new pre-amplifier with variable gain as prototype of DAQ based on NI hardware.

*XXII International Baldin Seminar on High Energy Physics Problems
15-20 September 2014
JINR, Dubna, Russia*

¹Speaker

1. Introduction

The main goal of the relativistic heavy-ion collisions studies at Nuclotron-based Ion Collider fAcility (NICA) and at Facility for Antiproton and Ion Research (FAIR) is to explore the properties of nuclear matter under extreme density and temperature conditions in the coming years. The study of the dense baryonic matter at Nuclotron (BM@N project) [1] is proposed as a first stage in the heavy-ion program at NICA [2,3]. The research program of BM@N project will be focused on the production of strange matter in heavy ion collisions at beam energies between 2 and 6 A·GeV [4]. These studies will be complimentary to the Compressed Baryonic Matter (CBM) project experimental program [5,6] for fixed target heavy ion collisions at FAIR in future.

The APDs are proposed for the light readout for Forward Wall Detector (FWD) and “shashlyk” electromagnetic calorimeter at the BM@N [1]. FWD will allow to detect the spectators and fragments for the precision improvement of the reaction plane reconstruction in the semi-central events needed for the measurements of flows, global polarizations of the hyperons etc. The lead-scintillator electromagnetic calorimeter of the “shashlyk” type will allow to measure the spatial position and energy of electrons and photons produced in heavy-ion collisions.

The Compressed Baryonic Matter (CBM) detector is being designed for the investigation of the properties of highly compressed baryonic matter. Projectile Spectator Detector (PSD) is a detector of non-interacting nucleons and fragments emitted at very low polar angles in forward direction in nucleus-nucleus collisions [7]. It will be used to determine the collision centrality and the orientation of an event plane.

The PSD is a full compensating modular lead-scintillator calorimeter, which provides very good and uniform energy resolution. The calorimeter comprises 44 individual modules, each consisting of 60 lead/scintillator layers with a surface of $20 \times 20 \text{ cm}^2$. The scintillation light is read out via wavelength shifting fibers by Multi-Avalanche Photo-Diodes (APD). The main advantages of APDs are: very compact sizes, low bias voltage, gain comparable to PMT, relative low price, insensitivity to magnetic field and absence of nuclear counter effect (due to the pixel structure). Generally, APDs have the following properties: pixel density about $10^4 - 2 \cdot 10^4 \text{ mm}^{-2}$, size of $3 \times 3 \text{ mm}^2$, high dynamical range of 5 – 15000 ph.e., photon detection efficiency of $\sim 15 \%$, high counting rate of $\sim 10^5 \text{ Hz}$.

The ion beam with very high intensity at the CBM experiment raises a question on the radiation resistance of the hadron calorimeter. The overall radiation dose deposited in the PSD and the neutron flux was simulated by FLUKA [8] with the use of realistic CBM and PSD geometry and material budget as for SIS100 and SIS300 [7]. While simulated radiation dose is not critical for scintillators, the most crucial effect is the photodetectors degradation caused by the neutron flux through the rear side of PSD calorimeter. According to FLUKA simulation this flux near the beam hole might achieve $10^{12} \text{ neutrons/cm}^2$ for beam energy 4 AGeV and about $4 \cdot 10^{12} \text{ neutrons/cm}^2$ for beam energy 35 AGeV and 2 months of CBM run at the beam rate 10^8 ions per second. Therefore, the main requirement for APDs for PSD CBM is the radiation hardness to neutron fluxes of $\sim 10^{13} \text{ n/cm}^2$.

2. Experimental setup and software

Complex experimental setup was applied for the APD hardness investigation. The setup consist of Static characteristics setup for investigation of internal structure of APD, LED calibration set-up for real-time APD gain calibration, Cosmic's rays test setup for investigation of APDs output connected to single detector lead-scintillation module. Those setups allow to study APDs comprehensively.

2.1 Setup for investigation of static characteristics

For our investigation, we used three general methods based on analysis of static characteristics, dynamic characteristics and APD operation. Static characteristics consist of Capacitance-Voltage (C-V), Capacitance-Frequency (C-F) and Current-Voltage (I-V) dependencies. Analysis of those characteristics allows to investigate the internal structure of APD, study of the behaviors of p-n junction during APD operation and measure the parameters of APD for equivalent circuit of APD in SPICE.

Static characteristics setup is shown in Figure 2.1. It consists of two following devices. Electrometer Keithley 6517A for current measurement in range 1fA – 20 mA, voltage measurement in range 10 μ V – 200 V \pm 10 – 1000 mV, biasing voltage supply in range up to 1000 V \pm 5 – 50 mV. LCR-meter Hioki 3532-50 for capacitance measurement in range 0.3 pF – 370 mF and frequency measurement in range 42 Hz – 5 MHz. These devices are connected to investigated APD and controlled via GPIB/USB interface by a dedicated PC software R.D.S.D. [9]. The R.D.S.D. software provides measurement of I-V, C-V and C-F characteristics in automatic mode for given ranges and increments of V or F correspondingly and has a feature of hysteresis measurement as well as simple analysis of measured data.

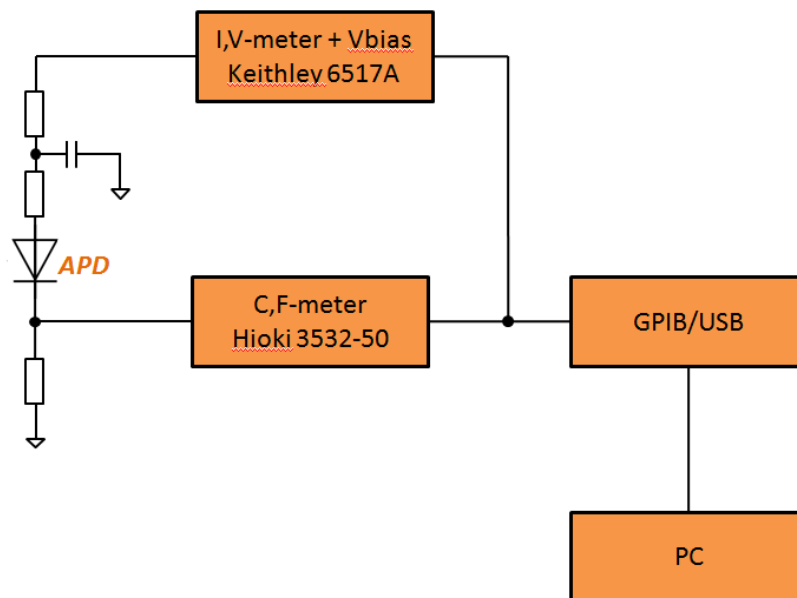


Figure 2.1: Static characteristics setup

2.2 LED calibration setup

The advantage of the light emitting diode (LED) light is that it can be easily tuned by width and intensity of the electrical pulse. The width of the pulse can be chosen to be close to

the width of the light pulse produced by shower (~ 10 ns) and the intensity in the suitable range to cover the dynamic range of the shower response in the cell. As shown in [10], “very good resolution of SiPMs and linearity at low light intensities enables to resolve single photon peaks and provides a unique opportunity to calibrate SiPM gain by a fit with a linear combination of Gaussians”. We will apply this method to our case of the MAPD readout.

LED calibration setup is shown in Figure 2.2. It consists of two following devices. Electrometer Keithley 6517A for voltage measurement in range $10 \mu\text{V} - 200 \text{V} \pm 10 - 1000 \text{mV}$, biasing voltage supply in ranges up to $1000 \text{V} \pm 5 - 50\text{mV}$. APD tester for dark current measurement in range $0 - 2 \text{mA}$, amplitude measurement of the output signal in range $0 - 5 \text{VDC} \pm 100 \mu\text{V}$, gain preamplifier in input signal range $10 - 500 \text{mV}$, temperature measurement in the range $-20 + 80 \text{ }^\circ\text{C} \pm 0.25^\circ \text{C}$, LED pulse driver allows to generate pulses of light $10, 20, 30 \text{ nS}$ length. Controlled Photon Source for generation of photon pulses with defined number of photons for a period of time by LED controlled by calibrated APD combined with thermo stabilization. These devices are connected to investigated APD and controlled via GPIB/USB interface by a dedicated PC software.

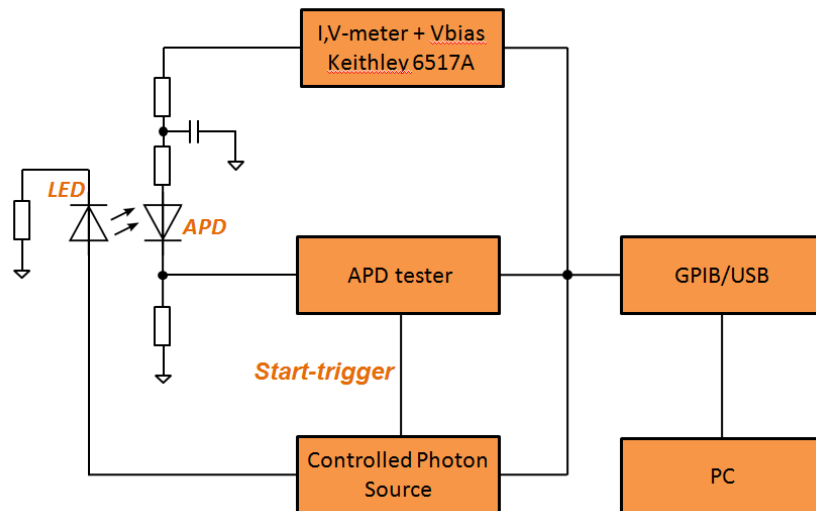


Figure 2.2: LED calibration setup

2.3 Cosmic rays test setup

Cosmic muons are a natural choice for the hadron calorimeter calibration, and they are used in all installed Cosmic rays test setups [11]. For the tests of the calibration system, a special prototype of the PSD module was assembled. It consist of only one section of the PSD module described in [7], i.e. a 12 cm long sandwich consisting of 6 layers of scintillator and lead. For the measurement of cosmic muons, the simple setup was arranged with two trigger scintillators of suitable size placed above and below the active section, see Fig.2.3.a. At the described conditions, the cosmic muons penetrate the PSD scintillators with path length in range of 16-200 mm (depending on their declination). The coincidence signal from two scintillators provided a trigger signal for DAQ, with frequency of about 10 counts per min. Therefore, a long acquisition time in order of days will be needed.

The response on the cosmic muons (passing in vertical direction) corresponds to one to few MIPs from target (passing PSD in horizontal plane). The Voltcraft PPS-12008 power supply was used as a HV supply for the MAPD optical sensor. The signal from the MAPD was

processed by a fast amplifier and the resulting pulse-height distribution was collected by the Yokogawa DL9240L oscilloscope. In addition, the similar measurement of cosmic muons was done with the PSD module at “vertical” position, when muons penetrate approximately a constant path of 24 mm (same as detected spectators in the real CBM experiments), see Fig.2.3.b.

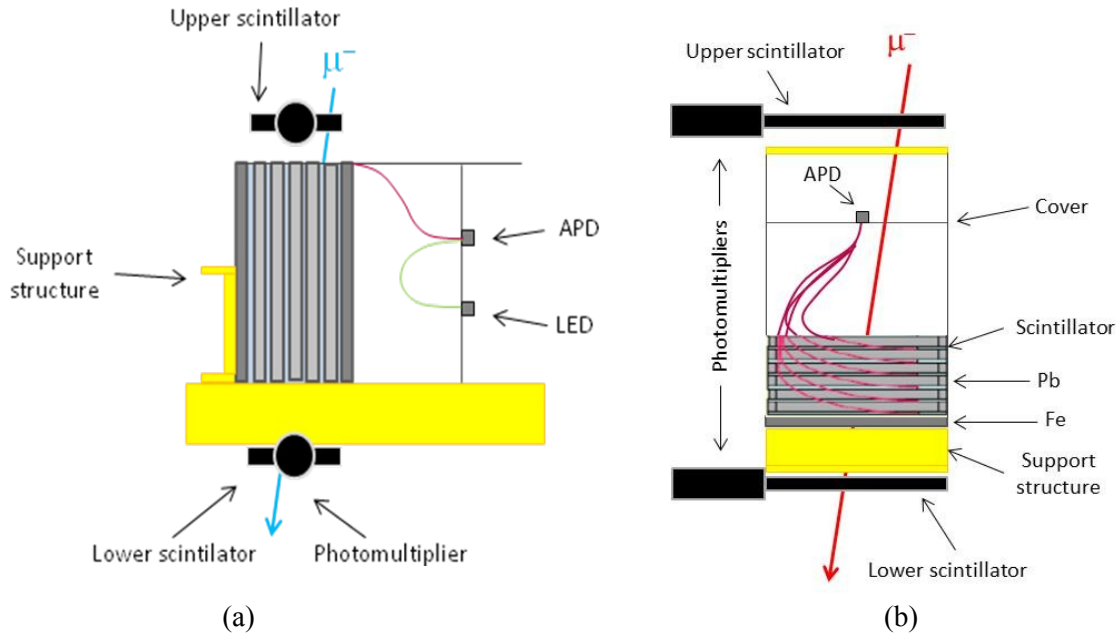


Figure 2.3: Cosmic ray test setup: a- horizontal setup; b - vertical setup

2.4 Monitoring during irradiation by neutrons at the Cyclotron facility

Tests at Cyclotron U120M at NPI Rez are aimed to conduct irradiation of Avalanche PhotoDiodes (APDs) with neutrons of maximal possible energy and several intensities varied in wide range to study radiation induced degradation of their main parameters with help of Fast neutron source. Considering the PSD detector design, the detector will operate in radiation conditions very close to white neutron spectrum that can be achieved with p+Be White Spectrum Source. APDs produced by the Ketek, Zecotek and Hamamatsu were measured. APDs were measured offline right after irradiation using dedicated measurement setups developed in our laboratory. During the next irradiation tests, APDs are planned also to be measured online during the irradiation and. Furthermore, the neutron beam fluence was measured during irradiation using the PIN-diode based Kerma-meter.

Online APD (SiPM) measurement setup is presented at Figure 2.4. It consists of: PIN diode BPW34 connected to Kerma Meter RM20 used for neutron fluence measurement [12], APD sample biased by voltage power supply from Keithley 6517A, APD tester [13] and Textronix oscilloscope for online measurement of APD diode parameters, TCP-IP/GPIB and TCP-IP/RS-232 converters for the data transfer and control from the control room. PIN diode BPW34 used for neutron fluence measurement and APD sample is placed in $\sim 3\text{m}$ distance from the neutron source to achieve the minimal possible intensity of neutron beam for the irradiation. All other equipment is placed behind the wall and connected to Ethernet cable going to control room. In addition, it is planned to measure the neutron beam profile using the 4 scintillators array with PMTs developed in collaboration with JINR group.

Already conducted test of Ketek [14] and Zecotek [15] APDs irradiation were done with p+7Li(C) Quasimonoenergetic Source and neutron dose of 3×10^{12} n/cm². It showed that the APDs damage is too high for these diodes to operate in the single photon mode [16].

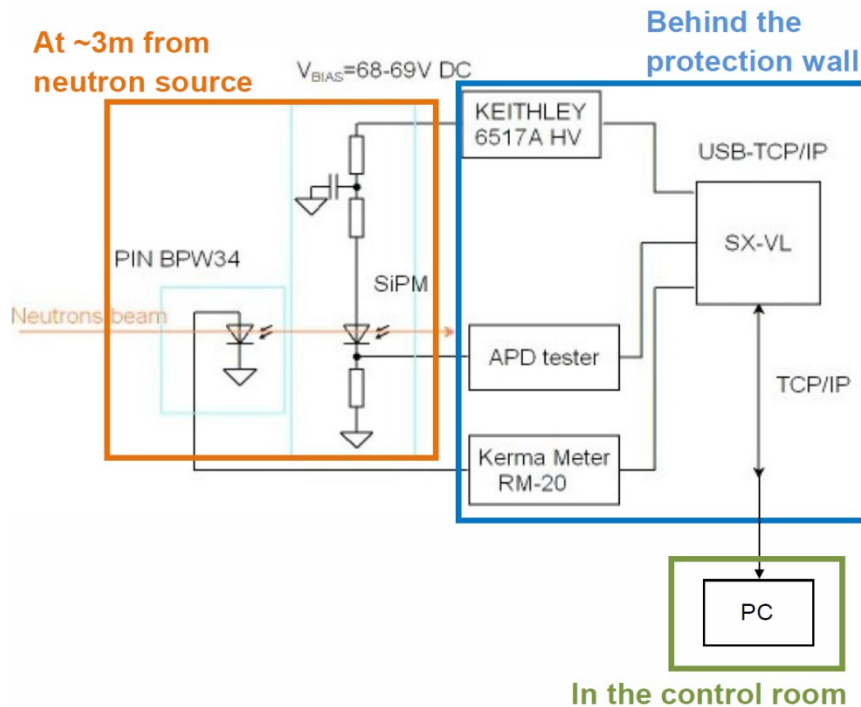


Figure 2.4: Online APD (SiPM) measurement setup

3. Data Analysis

3.1 Analysis of I-V, C-V and C-F characteristics

Investigation of static characteristics of semiconductor detectors is very important to understand the physics of internal processes occurring during the irradiation. Modern semiconductor detector is a device with a complex internal structure. During irradiation experiment this structure changes because external irradiation violate the equilibrium of lattice of the base material – Silicon. Different kinds of structural defects and high electric field inside the detector are the basic factors which are responsible for variation of Silicon's internal conductivity and lead to the destruction of Silicon's internal structure on a long time scale.

Capacitance-voltage C-V characteristic is a fundamental characteristic, which is usually carried out by the study of properties of semiconductor detectors [17]. The reverse-biased I-V characteristic of P-N junction provides information concerning the generation-recombination process in the silicon bulk. This characteristic allows to estimate the influence of irradiation on noise performance of the detector.

Investigated APDs were irradiated at the Cyclotron facility of NPI Rež using quasi-monoenergetic 35 MeV secondary neutron beam [9]. Single Zecotek APD was irradiated with dose of $3.4 \pm 0.2 \cdot 10^{12}$ n/cm² and two Ketek APDs were irradiated with dose of $2.5 \pm 0.2 \cdot 10^{12}$ n/cm². Doses here are measured by the special PIN diode calibrated for a 1 MeV neutrons equivalent dose; the temperature during the irradiation and measurements was 22 ± 0.5 °C [12].

C-V characteristics of Zecotek APDs are showing significant decrease of the hysteresis after irradiation (Figure 3.1, left). It can be related to decrease of long-living traps number in APD volume and therefore increase of short-living traps number, which is confirmed by C-F

measurements as well. C-V characteristics of Ketek APDs are showing significant restoration of the initial C-V dependence in 4 days after irradiation (Figure 3.1, right). However, even after self-annealing one can clearly see significant difference in C-V before and after irradiation related to in-volume radiation effects, especially close to operational voltage of 25 V.

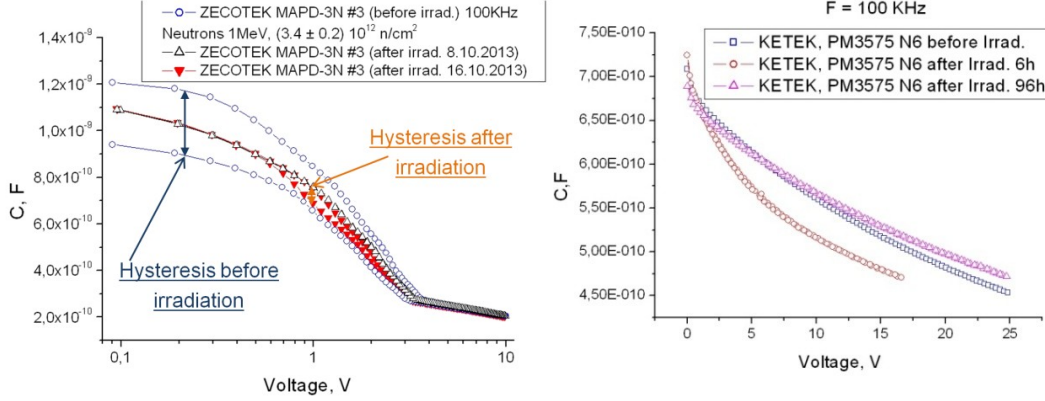


Figure 3.1: C-V characteristics of Zecotek (left) and Ketek (right) APDs before and after irradiation

C-F characteristic is more difficult to understand due to the lack of information about trap's centres in Silicon after irradiation. C-F shows the integral effect of multiple defects and it is not a simple task to analyse it. However, the simplest way of analysis is to achieve useful information in terms of mean values. We propose simple model describing behaviour of C-F characteristic depicted below. Dynamical process describing variation of nonequilibrium carriers due to recharge of traps' levels in silicon volume is depicted in [18]. Here it is presumed that measured capacitance C and geometrical capacitance are connected in parallel. For the measured capacitance C being bigger than geometrical one, variation of nonequilibrium carriers' concentration Δn is with lifetime τ is described by following equation:

$$\frac{\partial \Delta n}{\partial t} = \frac{1}{e} \cdot \frac{\partial J_n}{\partial x} + \frac{\Delta n}{\tau}$$

where e is elementary charge and J_n is the current through p-n junction.

Multiplying the left part by $\partial \varphi / \partial \varphi$ and e/e , substituting $\partial \Delta n$ by $\partial q \cdot e$ and assuming $\partial J_n / \partial x$ tending to zero due to small gradient of current across p-n junction, one can achieve:

$$\frac{\partial \Delta n}{\partial t} \cdot \frac{\partial \varphi}{\partial \varphi} \cdot \frac{e}{e} = \frac{\Delta n}{\tau} \Rightarrow \frac{\partial q}{\partial \varphi} \cdot \frac{\partial \varphi}{\partial t} = e \cdot \frac{\Delta n}{\tau}$$

Here we can move from ∂ increments tending to zero to small but measurable Δ increments: $\partial q \rightarrow \Delta q$, $\partial \varphi \rightarrow \Delta \varphi$, $\partial t \rightarrow \Delta t$, where $\Delta \varphi$ is voltage modulation applied to p-n junction for time Δt and inducing charge change Δq . Finally, substituting time interval Δt by frequency f to move from the time representation to frequency representation and substituting $\Delta q / \Delta \varphi$ by p-n junction capacitance C , one can achieve:

$$\frac{\Delta q}{\Delta \varphi} \cdot \frac{\Delta \varphi}{\Delta t} = e \cdot \frac{\Delta n}{\tau} \Rightarrow C \cdot \Delta \varphi \cdot f = e \cdot \frac{\Delta n}{\tau}$$

We assume that carriers' concentration Δn is proportionally equal to traps' levels concentration $\langle N_t \rangle$ as all the traps' level are ionised for the given temperature. Here, traps' levels concentration $\langle N_t \rangle$ and traps' levels lifetimes $\langle \tau \rangle$ are considered as averaged values for

all the different traps' levels in the p-n junction. Substituting Δn by $\langle N_t \rangle$ and τ by $\langle \tau \rangle$ we can rewrite achieved formula in final version as:

$$\frac{1}{C}(f) = \frac{1}{e} \cdot \frac{\langle \tau \rangle}{\langle N_t \rangle} \cdot \Delta \varphi \cdot f \quad (1)$$

Achieved equation (1) is describing the dependence of traps' levels in semiconductor volume on the capacitance of p-n junction and can be extremely useful for the C-F characteristics analysis.

C-F characteristics of both Zecotek and Ketek APDs are showing the capacitance increase for high frequencies and the capacitance decrease for low frequencies (Figure 3.2). Considering the $1/C \sim f$ model, this effect can be related respectively to the increase of short-living traps amount and the decrease of long-living traps amount. The delimiting value of traps lifetime to be considered as short- or long-living is $0.5 \mu\text{s}$ for Zecotek and $2.5 \mu\text{s}$ for Ketek.

Considering that e and $\Delta \varphi$ are constants and assuming $\langle N_t \rangle$ being less sensitive to the irradiation than $\langle \tau \rangle$ in (1), one can see that the less the traps lifetime τ , the less $1/C(f)$ is dependent on f . As the Figure 3.2 shows lower slope of $1/C(f)$ after irradiation, then the average traps lifetime should be decreasing.

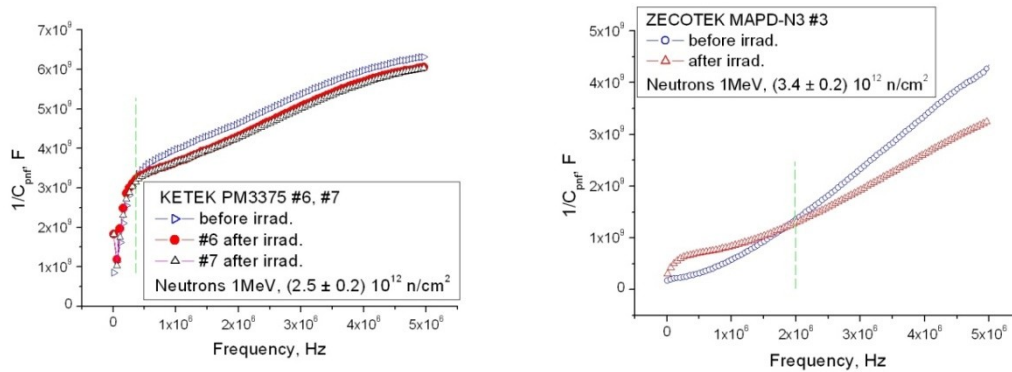


Figure 3.2: C-F characteristics of Zecotek (left) and Ketek (right) APDs before and after irradiation

3.2 Tests of APDs with LED and cosmic rays

Modern investigation of single-photon detectors is not possible without single-photon sources. Simple and reliable source of photons is Light Emitted Diode (LED). Main advantage of LED is possibility to apply the method of synchronous detection for APD tests of signal that allows to investigate APD after irradiation in single-photon mode of operation when signal to noise ratio is very low and can be calculated using big statistics of single photon events. This method allows to investigate threshold variation of APD photon detection. Cosmic rays are very good low cost replacement for conduction of actual experiment with APDs involving accelerator facilities. The disadvantage of this method is low data rate which is not of high importance on stage of R&D. Main advantage of cosmic rays is possibility to employ low cost high energy muons (MIP particles) to test APDs in generally any experimental laboratory with the same source of particles. Results of Zecotek and Ketek APDs tests with LED and cosmic rays before and after irradiation are presented at figures 3.3 and 3.4.

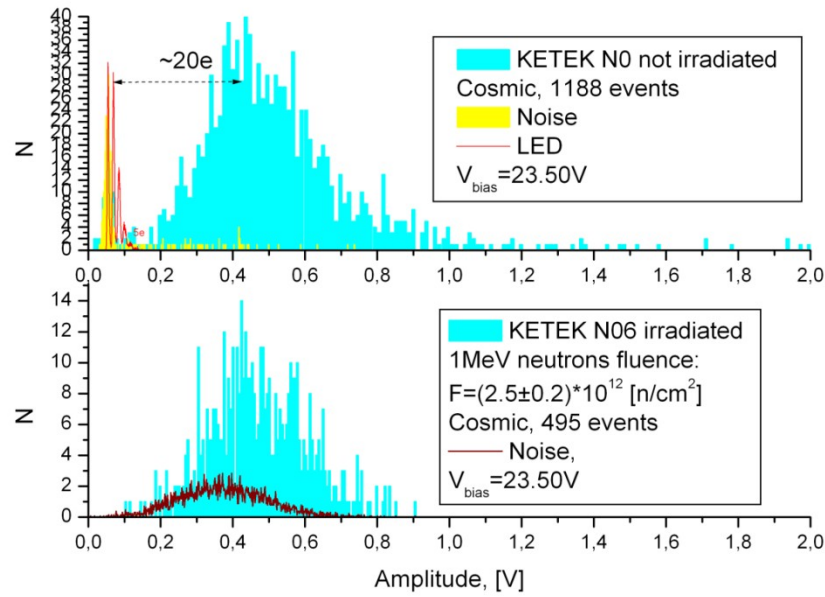


Figure 3.3: Ketek APD test with LED and cosmic muons before and after APD irradiation

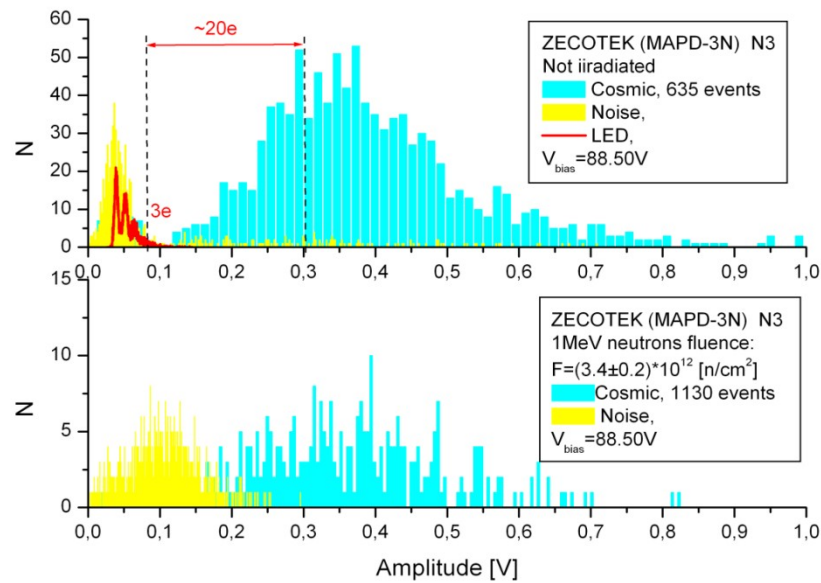


Figure 3.4: Zecotek APD test with LED and cosmic muons before and after APD irradiation

4. Conclusion

While many different irradiation effects were detected after the irradiation, all of them are mainly pointing to the increase of the APDs' internal noise. Especially, high frequency noise, which is directly dependent on the short-living traps amount in APD volume. Considering results of investigation we can conclude that APDs are not able to detect single photons anymore due to high noise levels.

The next steps will be a study of the radiation hardness of Ketek, Zecotek and Hamamatsu APDs with online dose monitoring, long time cosmic tests for all types of APDs and investigation of dependence of optimal avalanche amplification on absorbed radiation dose.

References

- [1] T.O. Ablyazimov et al. (BM@N Collaboration), Conceptual Design Report of BM@N, <http://nica.jinr.ru/files/BM@N/BMN-CDR.pdf>
- [2] V.D. Kekelidze, A.S. Sorin et al. (NICA Collaboration), Design and Construction of Nuclotron-based Ion Collider fAcility (NICA). Conceptual Design Report, <http://nica.jinr.ru>.
- [3] G. Musulmanbekov for NICA Collaboration, The NICA/MPD Project at JINR, Nucl. Phys. A862–863 (2011) 244.
- [4] V. Ladygin et al., Study of strange matter production in the heavy ion collisions at NUCLOTRON, in proceedings of the XXI-st International Baldin Seminar on High Energy Physics Problems: Relativistic Nuclear Physics and Quantum Chromodynamics (ISHEPP 2012), 10-15 September, 2012, Dubna, Russia, PoS(Baldin-ISHEPP-XXI)038 (2012).
- [5] B. Friman, C. Hohne, J. Kroll, S. Leupold, J. Randrup, R. Rapp and P. Senger, The CBM physics book: Compressed baryonic matter in laboratory experiments, Lect. Notes Phys. 814 (2011) 1.
- [6] The CBM experiment at FAIR facility, <http://www.fair-center.eu/public/experiment-program/nuclear-matter-physics/cbm.html>.
- [7] PSD Technical Design Report for the CBM Collaboration, version of March 2013.
- [8] T.T. Böhlen et al., “The FLUKA Code: Developments and Challenges for High Energy and Medical Applications”, Nuclear Data Sheets 120, 211-214 (2014).
- [9] V. Mikhaylov, V. Kushpil, Developing of the R.D.S.D. software for the research and analysis of radiation defects in semiconductor detectors in static and dynamic cases https://ojs.ujf.cas.cz/~wagner/transmutace/studentpraxe/mikhailov/Report_Mikhaylov6.doc.
- [10] J. Cvach, CALICE scintillator hadron calorimeter prototype commissioning and calibration, PRAMANA Journal of Physics 69 (6) (2007) 1031.
- [11] Performance of the CMS hadron calorimeter with cosmic ray muons and LHC beam data, CMS Collaboration, 2010, <http://iopscience.iop.org/1748-0221/5/03/T03012>.
- [12] V. Kushpil, S. Kushpil and Z. Huna, A simple device for the measurement of kerma based on commercial PIN photo diodes, EPJ Web of Conferences 24 (2012) 07008.
- [13] V. Kushpil, S. Kushpil, Universal single board tester for investigation of the avalanche photo detectors, JINST 7 (2012) C01084.
- [14] Ketek PM3350 Datasheet, <http://www.ketek.net/products/sipm/pm3350/>.
- [15] Zecotek WHITE PAPER MAPD Photo-Detectors, <http://www.zecotek.com/media/MAPD-WhitePaper-March-2011.pdf>.
- [16] V. Kushpil, V. Mikhaylov, S. Kushpil, P. Tlustý, O. Svoboda, A. Kugler, Radiation hardness investigation of avalanche photodiodes for the Projectile Spectator Detector readout at the Compressed Baryonic Matter experiment, doi:10.1016/j.nima.2014.11.071.
- [17] J. Hilibrand and R.D. Gold, Determination of the Impurity Distribution in Junction Diodes From Capacitance-Voltage Measurements, RCA Review, 21 (1960) 245.
- [18] E. Schibli and A. G. Milnes, Effects of deep impurities on n+p junction reverse-biased small-signal capacitance, Solid-State Electronics, 11 (1968) 323-334.